

30. DiAntonio, A., Parfitt, K. O. & Schwartz, T. L. Synaptic transmission persists in synaptotagmin mutants of *Drosophila*. *Cell* **73**, 1281–1290 (1993).
31. Martin, A. R. A further study of the statistical composition of the endplate. *J. Physiol.* **130**, 114–122 (1955).

Supplementary Information accompanies the paper on Nature's website (<http://www.nature.com/nature>).

## Acknowledgements

We thank I. Inman for technical assistance; N. Reist, J. Li Bryan Stewart and B. Niemeyer for reagents and discussions; and N. Gay and the Department of Biochemistry (Cambridge) for resources. I.M.R. was supported by the American Heart Association, Western Affiliate, and is a Medical Research Council Career Development Award Fellow. The work was supported by the Muscular Dystrophy Association, by a Silvio Conti Center for Neuroscience Award from the National Institute of Mental Health, and by the National Institutes of Health (T.L.S.).

## Competing interests statement

The authors declare that they have no competing financial interests.

Correspondence and requests for materials should be addressed to T.L.S. (e-mail: [thomas.schwarz@tch.harvard.edu](mailto:thomas.schwarz@tch.harvard.edu)) or I.M.R. (e-mail: [i.robinson@gen.cam.ac.uk](mailto:i.robinson@gen.cam.ac.uk)).

## The C<sub>2</sub>B Ca<sup>2+</sup>-binding motif of synaptotagmin is required for synaptic transmission *in vivo*

J. M. Mackler\*, J. A. Drummond†, C. A. Loewen\*, I. M. Robinson† & N. E. Reist\*

\* Department of Anatomy and Neurobiology, Program in Molecular, Cellular, and Integrative Neuroscience, Colorado State University, Fort Collins, Colorado 80523, USA

† Department of Genetics, University of Cambridge, Cambridge CB2 3EH, UK

Synaptotagmin is a synaptic vesicle protein that is postulated to be the Ca<sup>2+</sup> sensor for fast, evoked neurotransmitter release<sup>1</sup>. Deleting the gene for synaptotagmin (*syt<sup>null</sup>*) strongly suppresses synaptic transmission in every species examined<sup>2</sup>, showing that synaptotagmin is central in the synaptic vesicle cycle. The cytoplasmic region of synaptotagmin contains two C<sub>2</sub> domains, C<sub>2</sub>A and C<sub>2</sub>B. Five, highly conserved, acidic residues in both the C<sub>2</sub>A and C<sub>2</sub>B domains of synaptotagmin coordinate the binding of Ca<sup>2+</sup> ions<sup>3–5</sup>, and biochemical studies have characterized several *in vitro* Ca<sup>2+</sup>-dependent interactions between synaptotagmin and other nerve terminal molecules<sup>6</sup>. But there has been no direct evidence that any of the Ca<sup>2+</sup>-binding sites within synaptotagmin are required *in vivo*. Here we show that mutating two of the Ca<sup>2+</sup>-binding aspartate residues in the C<sub>2</sub>B domain (D<sub>416,418</sub>N in *Drosophila*) decreased evoked transmitter release by >95%, and decreased the apparent Ca<sup>2+</sup> affinity of evoked transmitter release. These studies show that the Ca<sup>2+</sup>-binding motif of the C<sub>2</sub>B domain of synaptotagmin is essential for synaptic transmission.

The C<sub>2</sub>B domain is critical for synaptotagmin function *in vivo*<sup>7–11</sup>, yet most of the Ca<sup>2+</sup>-dependent, biochemical interactions of synaptotagmin were originally mapped to the C<sub>2</sub>A domain<sup>12</sup>. Thus, the importance of Ca<sup>2+</sup> binding by the C<sub>2</sub>B domain has been largely neglected. The recent finding that the C<sub>2</sub>B domain mediates Ca<sup>2+</sup>-dependent interactions with phospholipids<sup>5,13</sup> has heightened interest in Ca<sup>2+</sup> binding by C<sub>2</sub>B. However, the effects of mutations of the acidic residues that coordinate Ca<sup>2+</sup> binding in the C<sub>2</sub>B domain have not been examined at intact synapses. We mutated the C<sub>2</sub>B aspartate residues to assess the importance of

the C<sub>2</sub>B Ca<sup>2+</sup>-binding motif. Specifically, we mutated the third and fourth aspartate residues that coordinate Ca<sup>2+</sup>-binding in the C<sub>2</sub>B domain of *Drosophila* synaptotagmin to asparagines (D<sub>416,418</sub>N, referred to henceforth as B-D<sub>3,4</sub>N, Fig. 1a) and expressed the mutant protein in a *syt<sup>null</sup>* line of *Drosophila*. Thus, the only source of synaptotagmin I in these lines (*P[syt<sup>B-D3,4N</sup>]*) was from the mutant transgene. As a negative control, we used the *syt<sup>null</sup>* line alone, and as a positive control, we used the same *syt<sup>null</sup>* line expressing synaptotagmin from a transgene bearing no mutations<sup>11</sup> (*P[syt<sup>WT</sup>]*).

Ca<sup>2+</sup>-evoked neurotransmitter release in *P[syt<sup>B-D3,4N</sup>]* mutant larvae was reduced to a level even less than that seen in the *syt<sup>null</sup>* negative control (Fig. 1b, c). Spontaneous and evoked potentials were recorded from third-instar muscle fibres as previously described<sup>14</sup>, except that evoked values were corrected for contamination by spontaneous release when appropriate<sup>15</sup> (see Supplementary Information). When motor nerves of third-instar larvae were stimulated in standard HL3 saline<sup>16</sup> containing 1.5 mM Ca<sup>2+</sup>, the mean amplitude of evoked excitatory junction potentials (EJPs) in muscles from *P[syt<sup>WT</sup>]* larvae was 25.0 ± 1.88 mV with no failures (*n* = 13), whereas mean EJP amplitude in *P[syt<sup>B-D3,4N</sup>]* larvae was only 0.21 ± 0.06 mV (*n* = 11) with a 78% failure rate. By comparison, mean EJP amplitude from *syt<sup>null</sup>* larvae was 1.70 ± 0.28 mV (*n* = 10) with a 15% failure rate.

In contrast to the decrease in evoked transmitter release, *P[syt<sup>B-D3,4N</sup>]* and *syt<sup>null</sup>* mutant synapses exhibited an increased rate of spontaneous vesicle fusion events (*P[syt<sup>WT</sup>]*, 2.9 ± 0.5 Hz; *P[syt<sup>B-D3,4N</sup>]*, 6.6 ± 1.4 Hz; *syt<sup>null</sup>*, 6.6 ± 0.8 Hz). The high frequency of miniature excitatory junction potentials (mEJPs) in mutant larvae shows that synaptic vesicles can fuse with the presynaptic membrane. The mean mEJP amplitudes for *P[syt<sup>B-D3,4N</sup>]* and *syt<sup>null</sup>* larvae were almost identical (0.99 ± 0.11 mV, *n* = 11 and 1.04 ± 0.08 mV, *n* = 10, respectively; *P* = 0.68), and slightly larger than that of *P[syt<sup>WT</sup>]* larvae (0.72 ± 0.09 mV, *n* = 11; *P* < 0.05). However, the frequency distribution curves of spontaneous mEJP amplitudes were remarkably similar among all genotypes (Fig. 1d), indicating that most vesicle fusions in all genotypes result in the same quantal sizes. The small number of larger events may represent either fusion of larger vesicles or an increased number of double and triple events owing to the increased mini frequency in the *syt<sup>null</sup>* and *P[syt<sup>B-D3,4N</sup>]* mutants. To further examine the fusibility of vesicles in *P[syt<sup>B-D3,4N</sup>]* mutant terminals, we focally applied a hypertonic solution (2.0 M sucrose) to elicit neurotransmitter release independent of nerve stimulation. Though variable, sucrose-stimulated release was comparable in *P[syt<sup>WT</sup>]* and *P[syt<sup>B-D3,4N</sup>]* larvae (Fig. 1e). Taken together, these data show that synaptic vesicles are capable of fusing with the presynaptic membrane. However, in *P[syt<sup>B-D3,4N</sup>]* mutants, nerve stimulation triggers the fusion of even fewer vesicles than in *syt<sup>null</sup>* mutants.

To determine the Ca<sup>2+</sup> dependence of neurotransmitter release, we measured EJP amplitude at extracellular Ca<sup>2+</sup> concentrations ranging from 0.4 to 5 mM for *P[syt<sup>WT</sup>]*, *P[syt<sup>B-D3,4N</sup>]* and *syt<sup>null</sup>* mutants (Fig. 1f). Although they differed greatly in maximal response, *P[syt<sup>WT</sup>]* and *syt<sup>null</sup>* fibres showed a similar Ca<sup>2+</sup> dependence (Fig. 1f, g), with values of EC<sub>50</sub> (effector concentration for half-maximum response) of 1.05 and 0.93 mM, respectively. The maximal response in *P[syt<sup>B-D3,4N</sup>]* fibres was reduced even more than in *syt<sup>null</sup>* fibres. Moreover, *P[syt<sup>B-D3,4N</sup>]* fibres showed a significantly shifted Ca<sup>2+</sup> dependence compared to *P[syt<sup>WT</sup>]* and *syt<sup>null</sup>*, with an EC<sub>50</sub> of 1.95 mM (Fig. 1f, g). To facilitate comparison of the *P[syt<sup>WT</sup>]* and *P[syt<sup>B-D3,4N</sup>]* mutants, the data were plotted as a percentage of the maximal response in each line (Fig. 1g). The rightward shift of the dose-response curve in the *P[syt<sup>B-D3,4N</sup>]* mutants shows that the apparent Ca<sup>2+</sup> affinity of synaptic transmission is reduced by the B-D<sub>3,4</sub>N mutation.

As evoked release was even lower in *P[syt<sup>B-D3,4N</sup>]* mutants than in *syt<sup>null</sup>* mutants, we examined whether the mutant protein dom-

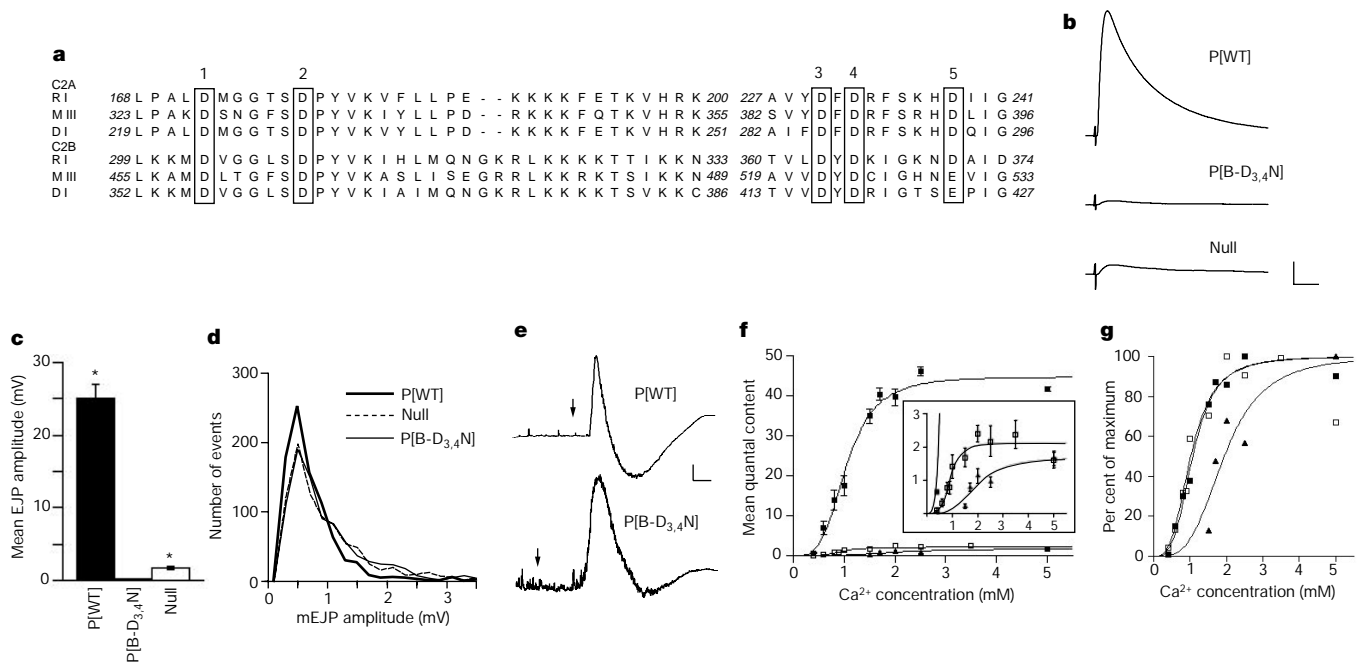


**Figure 1** Fast, Ca<sup>2+</sup>-evoked synaptic transmission is nearly abolished, and the apparent Ca<sup>2+</sup> affinity of evoked transmitter release is decreased, in a C<sub>2</sub>B Ca<sup>2+</sup>-binding motif mutant. **a**, Partial amino-acid sequence of C<sub>2</sub>A and C<sub>2</sub>B domains of rat *syt I* (R I), mouse *syt III* (M III), and *Drosophila syt I* (D I). The five conserved acidic residues that coordinate the binding of multiple Ca<sup>2+</sup> ions are boxed. **b**, Averages of 30 evoked excitatory junction potentials (EJPs) recorded in saline containing 1.5 mM Ca<sup>2+</sup>. P[WT], *syt*<sup>null</sup> expressing the P[*syt*<sup>WT</sup>] transgene; P[B-D<sub>3,4</sub>N], *syt*<sup>null</sup> expressing the P[*syt*<sup>B-D<sub>3,4</sub>N</sup>] transgene; Null, *syt*<sup>null</sup>. Scale bars: 5 mV, 20 ms. **c**, Mean EJP amplitude ± s.e.m. Asterisks indicate results that are significantly different from P[B-D<sub>3,4</sub>N] (*P* < 0.001, Satterthwaite *t*-test).

**d**, Frequency distribution curves of miniature EJP (mEJP) amplitudes calculated from 850 individual events from each line compiled into 0.2-mV bins. **e**, Representative responses from P[WT] and P[B-D<sub>3,4</sub>N] fibres to focal application (arrows) of 2.0 M sucrose. Scale bars: 5 mV, 1.25 s. **f**, Linear plot of [Ca<sup>2+</sup>] versus mean quantal content. Each point represents the mean quantal content of 6–10 muscle fibres from ≥3 larvae. Filled squares, P[*syt*<sup>WT</sup>]; open squares, *syt*<sup>null</sup>; triangles, P[*syt*<sup>B-D<sub>3,4</sub>N</sup>]. Error bars where visible indicate s.e.m. Inset: enlarged to show P[*syt*<sup>B-D<sub>3,4</sub>N</sup>] and *syt*<sup>null</sup> curves. **g**, Ca<sup>2+</sup> dose response data normalized to illustrate the rightward shift of the P[*syt*<sup>B-D<sub>3,4</sub>N</sup>] curve. Symbols as in **f**.

inantly inhibits synaptic transmission. We analysed evoked release in larvae that coexpressed native synaptotagmin and the transgenic B-D<sub>3,4</sub>N mutant synaptotagmin. The control line only expressed synaptotagmin from the native gene, and not from the mutant transgene (see Supplementary Information). Under standard recording conditions, the control line (wild type, WT, Fig. 2a, b) displayed a mean EJP amplitude of 42.8 mV ± 1.1 (*n* = 9). In contrast, evoked transmitter release in larvae expressing both the native and the B-D<sub>3,4</sub>N mutant synaptotagmin (WT with B-D<sub>3,4</sub>N,

Fig. 2a, b) was reduced by 53% to 20.3 ± 3.2 mV (*n* = 11, *P* < 0.001). Thus, the B-D<sub>3,4</sub>N mutant protein inhibited synaptic transmission even in the presence of wild-type synaptotagmin. We also mutated the first and second of the aspartate residues that coordinate Ca<sup>2+</sup>-binding in the C<sub>2</sub>B domain to asparagines (D<sub>356,362</sub>N, referred to henceforth as B-D<sub>1,2</sub>N, Fig. 1a). However, when crossed into the *syt*<sup>null</sup> background, none of the embryos bearing the B-D<sub>1,2</sub>N mutant transgene were able to hatch. The late embryonic lethality suggests that the B-D<sub>1,2</sub>N mutation may be even

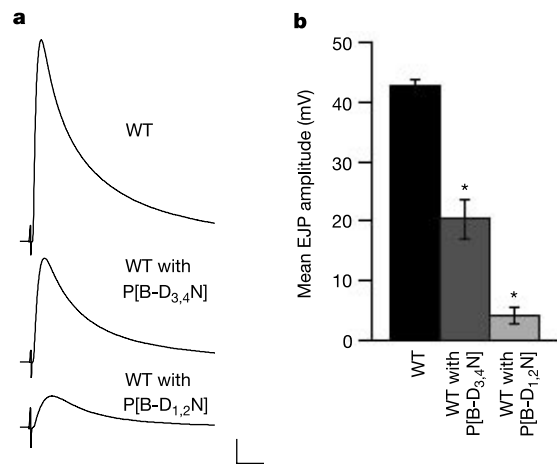


**Figure 2** Expression of B-D<sub>3,4</sub>N or B-D<sub>1,2</sub>N mutant synaptotagmin inhibits synaptic transmission in otherwise wild-type synapses. **a**, Average of 30 evoked EJPs from three genotypes: WT, a line heterozygous for the native *syt* gene which contains the P[*syt*<sup>B-D<sub>3,4</sub>N</sup>] transgene but lacks transgene expression; WT with P[B-D<sub>3,4</sub>N], a *syt*

heterozygote that expresses the B-D<sub>3,4</sub>N mutant protein; WT with P[B-D<sub>1,2</sub>N], a *syt* heterozygote that expresses the B-D<sub>1,2</sub>N mutant protein. Scale bars: 5 mV, 20 ms. **b**, Mean EJP amplitude ± s.e.m. for all three lines. Results that are significantly different from WT are indicated by asterisks (*P* < 0.001, Satterthwaite *t*-test).

more detrimental to the organism than the B-D<sub>3,4</sub>N mutation. Physiological analysis of larvae that coexpressed native synaptotagmin and the transgenic B-D<sub>1,2</sub>N mutant synaptotagmin (WT with P[B-D<sub>1,2</sub>N], Fig. 2a, b) support this hypothesis. The B-D<sub>1,2</sub>N mutant protein inhibited evoked transmitter release by at least 90.5% (4.09 ± 1.33 mV, n = 9, P < 0.0001) in the presence of wild-type synaptotagmin. The only common feature between these mutations is that each is lacking two of the aspartate residues that coordinate Ca<sup>2+</sup> binding in the C<sub>2</sub>B domain of synaptotagmin. Thus, two independent mutations that disrupt the Ca<sup>2+</sup>-binding motif of C<sub>2</sub>B each inhibit evoked transmitter release at *Drosophila* synapses.

To verify transgene expression in the *syt*<sup>null</sup> background, we stained P[*syt*<sup>WT</sup>] and P[*syt*<sup>B-D<sub>3,4</sub>N</sup>] larval whole mounts (Fig. 3a) and western blots of larval central nervous systems (CNS, Fig. 3b) with an anti-synaptotagmin antibody<sup>14</sup>. Both demonstrated abundant transgene expression. Thus in the *syt*<sup>null</sup> background, the B-D<sub>3,4</sub>N mutant protein is stably expressed in the larval nervous system and is appropriately targeted to neuromuscular junctions. To demonstrate transgene expression in the *syt* heterozygous background, similar western blots were analysed from the following lines: WT with P[*syt*<sup>B-D<sub>3,4</sub>N</sup>], WT with P[*syt*<sup>B-D<sub>1,2</sub>N</sup>], and their paired WT controls, each of which carry a transgene but do not express it (see Supplementary Information). Figure 3c shows that both of the transgene expressing lines (lanes 1 and 3) expressed

similar levels of synaptotagmin, whereas the control lines (lanes 2 and 4) expressed significantly less. Thus the mutant transgenes are also expressed in the *syt* heterozygous background. Coupled with the finding that evoked release was even lower in P[*syt*<sup>B-D<sub>3,4</sub>N</sup>] mutants than in *syt*<sup>null</sup> mutants (which exhibit no detectable synaptotagmin expression<sup>14</sup>), the expression data suggest that the electrophysiological deficits observed in these C<sub>2</sub>B Ca<sup>2+</sup>-binding motif mutants are unlikely to be a result of insufficient expression or mislocalization of the mutant transgenic protein.

The C<sub>2</sub>B domain of synaptotagmin has been proposed to take part in vesicle recycling<sup>17</sup>. This hypothesis is supported by ultra-

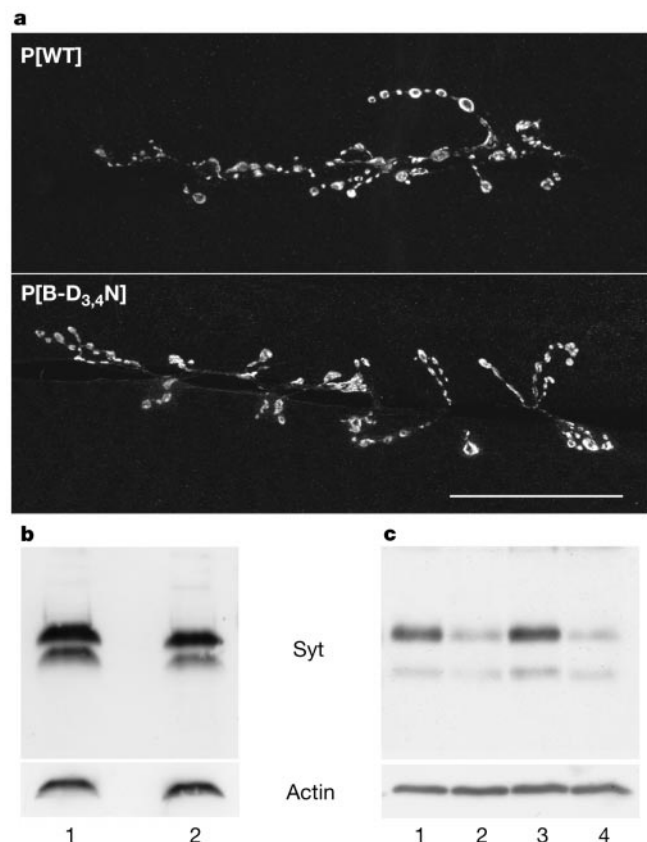


**Figure 3** Synaptotagmin expression in the nervous system of P[*syt*<sup>WT</sup>], P[*syt*<sup>B-D<sub>3,4</sub>N</sup>] and P[*syt*<sup>B-D<sub>1,2</sub>N</sup>] transgenic lines. **a**, Anti-synaptotagmin immunolabelling of P[*syt*<sup>WT</sup>] and P[*syt*<sup>B-D<sub>3,4</sub>N</sup>] larvae shows that the wild-type and mutant transgenes are both abundantly expressed at neuromuscular junctions, the synapse used for all analyses. Scale bar, 50 μm. **b**, Western blot showing synaptotagmin expression (seen as a doublet in *Drosophila*<sup>26</sup>) in the CNS of *syt*<sup>null</sup> larvae bearing *synaptotagmin* transgenes. Lane 1, P[*syt*<sup>WT</sup>]; lane 2, P[*syt*<sup>B-D<sub>3,4</sub>N</sup>]. **c**, Western blot showing *synaptotagmin* transgene expression in *syt* heterozygotes. Lane 1, WT with P[B-D<sub>3,4</sub>N]; lane 2, WT without P[B-D<sub>3,4</sub>N] expression; lane 3, WT with P[B-D<sub>1,2</sub>N]; lane 4, WT without P[B-D<sub>1,2</sub>N] expression.

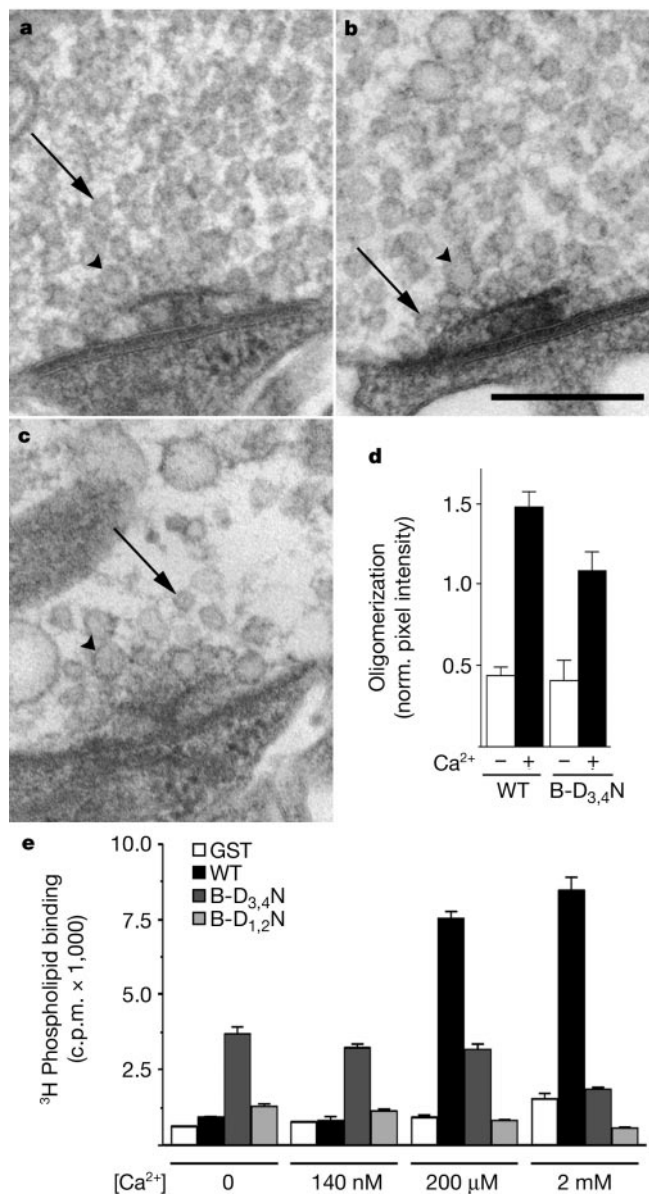


**Figure 4** Whereas defects in recycling and Ca<sup>2+</sup>-dependent oligomerization cannot account for the severe decrease in synaptic transmission, decreased Ca<sup>2+</sup>-dependent phospholipid binding may account for this. Representative nerve terminals from neuromuscular junctions of P[*syt*<sup>WT</sup>] (**a**), P[*syt*<sup>B-D<sub>3,4</sub>N</sup>] (**b**), and *syt*<sup>null</sup> (**c**) third-instar larvae. Although there is an increase in the number of large vesicles (arrowheads), synaptic vesicles (arrows) are abundant in P[*syt*<sup>B-D<sub>3,4</sub>N</sup>] mutant nerve terminals. Scale bar, 250 nm. **d**, Ca<sup>2+</sup>-dependent oligomerization was decreased by ~25% in C<sub>2</sub>A-C<sub>2</sub>B domains bearing the B-D<sub>3,4</sub>N mutation (mean ± s.e.m.). **e**, Ca<sup>2+</sup>-dependent phospholipid binding to GST-C<sub>2</sub>B is severely reduced or abolished by the B-D<sub>3,4</sub>N or B-D<sub>1,2</sub>N mutation, respectively (GST, glutathione *S*-transferase). Background liposome binding is shown in the GST alone columns.

structural observations of *sytn<sup>null</sup>* mutants<sup>18,19</sup>; first-instar *sytn<sup>null</sup>* mutants exhibit substantial depletion of synaptic vesicles and increased numbers of large vesicles, consistent with impaired recycling. If the electrophysiological deficits in our C<sub>2</sub>B Ca<sup>2+</sup>-binding motif mutants were the result of a recycling defect, one would expect *P[sytn<sup>B-D3,4N</sup>]* mutant terminals (Fig. 4b) to exhibit at least as much vesicle depletion as *sytn<sup>null</sup>* mutant terminals (Fig. 4c). Qualitative observation of synaptic ultrastructure revealed that the *P[sytn<sup>B-D3,4N</sup>]* mutants did exhibit some increase in large vesicles compared to controls (Fig. 4a, b); however, the abundance of synaptic vesicles in *P[sytn<sup>B-D3,4N</sup>]* mutant terminals suggests that recycling is not the main defect in these mutants. Because the >95% decrease in evoked transmitter release in the *P[sytn<sup>B-D3,4N</sup>]* mutant is not due to an absence of synaptic vesicles, the decreased release is probably a result of decreased release probability per vesicle.

In order to address the molecular mechanisms that may underlie the marked decrease in synaptic transmission caused by mutations in the C<sub>2</sub>B Ca<sup>2+</sup>-binding motif, we tested wild-type and mutant *Drosophila* synaptotagmin I for Ca<sup>2+</sup>-dependent interactions *in vitro*. Syntaxin binding by the C<sub>2</sub>B domain was not Ca<sup>2+</sup> dependent<sup>20</sup>, and the C<sub>2</sub>B Ca<sup>2+</sup>-binding motif mutations did not alter this interaction (data not shown). As previously seen for rat synaptotagmin<sup>9</sup>, we found that the B-D<sub>3,4</sub>N mutation caused a 25% reduction in Ca<sup>2+</sup>-dependent oligomerization (Fig. 4d, *P* = 0.052). Unlike the studies of the rat protein, however, the Ca<sup>2+</sup>-independent oligomerization was unchanged by the mutation. Ca<sup>2+</sup>-dependent phospholipid binding by the C<sub>2</sub>B domain<sup>5,13</sup>, on the other hand, was notably altered by the C<sub>2</sub>B Ca<sup>2+</sup>-binding motif mutations (Fig. 4e). Compared to wild type, the B-D<sub>3,4</sub>N mutation reduced Ca<sup>2+</sup>-dependent phospholipid binding by 65% at 200 μM Ca<sup>2+</sup> and by 95% at 2 mM Ca<sup>2+</sup> (*P* < 0.001), while increasing Ca<sup>2+</sup>-independent binding. The B-D<sub>1,2</sub>N mutation reduced Ca<sup>2+</sup>-dependent phospholipid binding even more severely, down to levels similar to background binding to glutathione *S*-transferase (GST) alone (Fig. 4e). These mutations have also been shown to disrupt Ca<sup>2+</sup>-dependent interactions between rat *sytn I* and phospholipids<sup>21</sup>. Both the oligomerization assay and the phospholipid-binding assay show that the C<sub>2</sub>B Ca<sup>2+</sup>-binding motif mutations disrupt Ca<sup>2+</sup>-dependent interactions of synaptotagmin.

The decreases in Ca<sup>2+</sup>-dependent phospholipid binding by the mutant C<sub>2</sub>B domains closely reflect the severity of the electrophysiological deficits seen *in vivo*. The B-D<sub>3,4</sub>N mutation severely decreased Ca<sup>2+</sup>-dependent phospholipid binding, and the B-D<sub>1,2</sub>N mutation completely blocked it. This correlation suggests that Ca<sup>2+</sup>-dependent phospholipid binding by the C<sub>2</sub>B domain may be a critical step in evoked transmitter release. Ca<sup>2+</sup>-dependent phospholipid binding by the C<sub>2</sub>A domain is also thought to be important for evoked transmitter release. A mutation in the C<sub>2</sub>A domain that decreased synaptotagmin's phospholipid binding *in vitro* also decreased evoked transmitter release<sup>22</sup>. However, alterations of the C<sub>2</sub>A Ca<sup>2+</sup>-binding motif do not appear to inhibit evoked release *in vivo*<sup>23</sup>. As the Ca<sup>2+</sup>-binding pockets of each C<sub>2</sub> domain are located in close proximity to one another<sup>4,24</sup>, Ca<sup>2+</sup> binding by the C<sub>2</sub>B domain may facilitate membrane binding by the C<sub>2</sub>A domain. Regardless of whether the C<sub>2</sub>A and C<sub>2</sub>B domains function cooperatively, our data—showing that mutation of two aspartates in C<sub>2</sub>B inhibited evoked transmitter release by >95%—demonstrate that the C<sub>2</sub>B Ca<sup>2+</sup>-binding motif is central to synaptotagmin function. Because synaptic vesicles in the *P[sytn<sup>B-D3,4N</sup>]* mutant terminals were plentiful and fusion-competent, the dramatic decrease in evoked release is unlikely to result from a vesicle recycling or biogenesis defect. These results are (to our knowledge) the first to show a disruption of synaptic transmission caused by mutation of a Ca<sup>2+</sup>-binding motif, and demonstrate that the C<sub>2</sub>B Ca<sup>2+</sup>-binding motif of synaptotagmin is essential for synaptic transmission *in vivo*. □

## Methods

### Site-directed mutagenesis and fly strains

Mutant *Drosophila sytn I* complementary DNA was generated by polymerase chain reaction (PCR) and used to transform *Drosophila* (see Supplementary Information). Either C<sub>2</sub>B aspartate residues 416 and 418 (Fig. 1a, residues labelled 3 and 4) or 356 and 362 (Fig. 1a, residues labelled 1 and 2) were mutated to asparagines. *sytn<sup>AD4</sup>* is a null mutation in the *Drosophila sytn I* gene<sup>25</sup>. We used a homozygous *sytn<sup>AD4</sup>* line, designated *sytn<sup>null</sup>*, as the negative control. The transgenic lines used include: *P[sytn<sup>WT</sup>]*; *P[sytn<sup>B-D3,4N</sup>]*; WT with *P*[B-D<sub>3,4</sub>N]; and WT with *P*[B-D<sub>1,2</sub>N] (see Supplementary Information for genotypes).

### Electrophysiology

Spontaneous and evoked potentials were recorded from third-instar muscle fibres as previously described<sup>14</sup> in standard HL3 saline<sup>16</sup> containing 1.5 mM Ca<sup>2+</sup> unless otherwise indicated. For Ca<sup>2+</sup> dose-response experiments, preparations were bathed in HL3 containing from 0.4 mM to 5 mM Ca<sup>2+</sup> (without adjusting Mg<sup>2+</sup>). Transmitter release was also evoked by focal application of a hypertonic, 2.0 M sucrose solution to fibres in standard HL3 saline. To prevent overestimating nerve-evoked transmitter release in *sytn<sup>null</sup>* and *P[sytn<sup>B-D3,4N</sup>]* larvae, we restricted the measurement interval for EJP amplitudes and subtracted an estimate of the spontaneous release<sup>15</sup> (see Supplementary Information). Failure rate was calculated as previously described<sup>26</sup>.

### Oligomerization

Soluble C<sub>2</sub>A-C<sub>2</sub>B domains were assayed for binding to immobilized GST-C<sub>2</sub>A-C<sub>2</sub>B domains according to the procedures of ref. 9 (see also Supplementary Information). Binding was wild type to wild type or mutant to mutant in buffer containing 2.5 mM CaCl<sub>2</sub> with or without 5 mM EGTA. Protein levels were quantified on Coomassie-blue-stained gels by comparison with bovine serum albumin (BSA) standards and were normalized to 12% of the total soluble protein used in the assay. There was no binding to GST alone. Binding assays were carried out three times.

### Lipid binding

Lipid binding was assayed by the binding of liposomes to GST-C<sub>2</sub>B fusion proteins<sup>27</sup>. Recombinant protein bound to glutathione agarose beads was mixed with tritiated PS/PC liposomes (see Supplementary Information) in test solutions containing EGTA and CaCl<sub>2</sub> to give the desired free [Ca<sup>2+</sup>]. Liposome binding was quantified by scintillation counting. Data points were obtained in triplicate. Data shown are representative of three separate experiments.

### Other techniques

Generation of recombinant proteins, western blot analysis, immunohistochemistry and electron microscopy experiments were carried out using standard techniques (see Supplementary Information).

Received 10 January; accepted 24 April 2002; doi:10.1038/nature00846.

Published online 7 July 2002.

- Augustine, G. J. How does calcium trigger neurotransmitter release? *Curr. Opin. Neurobiol.* **11**, 320–326 (2001).
- Lin, R. C. & Scheller, R. H. Mechanisms of synaptic vesicle exocytosis. *Annu. Rev. Cell Dev. Biol.* **16**, 19–49 (2000).
- Shao, X., Davletov, B. A., Sutton, R. B., Sudhof, T. C. & Rizo, J. Bipartite Ca<sup>2+</sup>-binding motif in C<sub>2</sub> domains of synaptotagmin and protein kinase C. *Science* **273**, 248–251 (1996).
- Sutton, R. B., Ernst, J. A. & Brunger, A. T. Crystal structure of the cytosolic C<sub>2</sub>A-C<sub>2</sub>B domains of synaptotagmin III: Implications for Ca<sup>2+</sup>-independent SNARE complex interaction. *J. Cell Biol.* **147**, 589–598 (1999).
- Fernandez, I. et al. Three-dimensional structure of the synaptotagmin I C<sub>2</sub>B-domain: Synaptotagmin I as a phospholipid binding machine. *Neuron* **32**, 1057–1069 (2001).
- Rizo, J. & Südhof, T. C. Domains, structure and function of a universal Ca<sup>2+</sup>-binding domain. *J. Biol. Chem.* **273**, 15879–15882 (1998).
- Bommert, K. et al. Inhibition of neurotransmitter release by C<sub>2</sub>-domain peptides implicates synaptotagmin in exocytosis. *Nature* **363**, 163–165 (1993).
- Fukuda, M. et al. Role of the C<sub>2</sub>B domain of synaptotagmin in vesicular release and recycling as determined by specific antibody injection into the squid giant synapse preterminal. *Proc. Natl Acad. Sci. USA* **92**, 10708–10712 (1995).
- Desai, R. C. et al. The C<sub>2</sub>B domain of synaptotagmin is a Ca<sup>2+</sup>-sensing module essential for exocytosis. *J. Cell Biol.* **150**, 1125–1136 (2000).
- Littleton, J. T. et al. *synaptotagmin* mutants reveal essential functions for the C<sub>2</sub>B domain in Ca<sup>2+</sup>-triggered fusion and recycling of synaptic vesicles *in vivo*. *J. Neurosci.* **21**, 1421–1433 (2001).
- Mackler, J. M. & Reist, N. E. Mutations in the second C<sub>2</sub> domain of synaptotagmin disrupt synaptic transmission at *Drosophila* neuromuscular junctions. *J. Comp. Neurol.* **436**, 4–16 (2001).
- Li, C. et al. Ca<sup>2+</sup>-dependent and -independent activities of neural and non-neural synaptotagmins. *Nature* **375**, 594–599 (1995).
- Bai, J., Wang, P. & Chapman, E. R. C<sub>2</sub>A activates a cryptic Ca<sup>2+</sup>-triggered membrane penetration activity within the C<sub>2</sub>B domain of synaptotagmin I. *Proc. Natl Acad. Sci. USA* **99**, 1665–1670 (2002).
- Loewen, C. A., Mackler, J. M. & Reist, N. E. *Drosophila synaptotagmin I* null mutants survive to early adulthood. *Genesis* **31**, 30–36 (2001).
- Petersen, S. A., Fetter, R. D., Noordermeer, J. N., Goodman, C. S. & DiAntonio, A. Genetic analysis of glutamate receptors in *Drosophila* reveals a retrograde signal regulating presynaptic transmitter release. *Neuron* **19**, 1237–1248 (1997).
- Stewart, B. A., Atwood, H. L., Renger, J. J., Wang, J. & Wu, C.-F. Improved stability of *Drosophila* larval neuromuscular preparations in haemolymph-like physiological solutions. *J. Comp. Physiol. A* **175**, 179–191 (1994).
- Zhang, J. Z., Davletov, B. A., Sudhof, T. C. & Anderson, R. G. Synaptotagmin I is a high affinity

- receptor for clathrin AP-2: implications for membrane recycling. *Cell* **78**, 751–760 (1994).
18. Jørgensen, E. M. *et al.* Defective recycling of synaptic vesicles in synaptotagmin mutants of *Caenorhabditis elegans*. *Nature* **378**, 196–199 (1995).
  19. Reist, N. E. *et al.* Morphologically docked synaptic vesicles are reduced in synaptotagmin mutants of *Drosophila*. *J. Neurosci.* **18**, 7662–7673 (1998).
  20. Kee, Y. & Scheller, R. H. Localization of synaptotagmin-binding domains on syntaxin. *J. Neurosci.* **16**, 1975–1981 (1996).
  21. Earles, C. A., Bai, J., Wang, P. & Chapman, E. R. The tandem C2 domains of synaptotagmin contain redundant Ca<sup>2+</sup> binding sites that cooperate to engage t-SNAREs and trigger exocytosis. *J. Cell Biol.* **154**, 1117–1123 (2001).
  22. Fernandez-Chacon, R. *et al.* Synaptotagmin I functions as a calcium regulator of release probability. *Nature* **410**, 41–49 (2001).
  23. Robinson, I. M., Ranjan, R. & Schwarz, T. L. Synaptotagmins I and IV promote transmitter release independently of Ca<sup>2+</sup> binding in the C<sub>2</sub>A domain. *Nature* advance online publication, 7 July 2002 (doi:10.1038/nature00915).
  24. Garcia, R. A., Forde, C. E. & Godwin, H. A. Calcium triggers an intramolecular association of the C2 domains in synaptotagmin. *Proc. Natl Acad. Sci. USA* **97**, 5883–5888 (2000).
  25. DiAntonio, A., Parfitt, K. D. & Schwarz, T. L. Synaptic transmission persists in synaptotagmin mutants of *Drosophila*. *Cell* **73**, 1281–1290 (1993).
  26. Del Castillo, J. & Katz, B. Quantal components of the end-plate potential. *J. Physiol.* **124**, 560–573 (1954).
  27. Davletov, B. A. & Sudhof, T. C. A single C<sub>2</sub> domain from synaptotagmin I is sufficient for high affinity Ca<sup>2+</sup>/phospholipid binding. *J. Biol. Chem.* **268**, 26386–26390 (1993).
  28. Littleton, J. T., Bellen, H. J. & Perin, M. S. Expression of synaptotagmin in *Drosophila* reveals transport and localization of synaptic vesicles to the synapse. *Development* **118**, 1077–1088 (1993).

Supplementary Information accompanies the paper on Nature's website (<http://www.nature.com/nature>).

## Acknowledgements

We thank S. Royer, C. Williams and K. Mace for technical assistance, and R. Handa, K. Beam, J. Herbers, M. Tamkun and R. Aldrich for discussions about this manuscript. This work was supported by the National Science Foundation (N.E.R.), the Muscular Dystrophy Association (N.E.R.), the March of Dimes (N.E.R.) and an MRC Career Development Award (I.M.R.).

## Competing interests statement

The authors declare that they have no competing financial interests.

Correspondence and requests for materials should be addressed to N.E.R. (e-mail: reist@lamar.colostate.edu).

# Calorie restriction extends *Saccharomyces cerevisiae* lifespan by increasing respiration

Su-Ju Lin\*, Matt Kaeberlein\*†, Alex A. Andalis‡, Lori A. Sturtz§, Pierre-Antoine Defossez\*†, Valeria C. Culotta§, Gerald R. Fink‡ & Leonard Guarente\*

\* Department of Biology, Massachusetts Institute of Technology, Cambridge, Massachusetts 02139, USA

‡ Whitehead Institute for Biomedical Research, Massachusetts Institute of Technology, Cambridge, Massachusetts 02142, USA

§ Department of Environmental Health Sciences, Johns Hopkins University School of Public Health, Baltimore, Maryland 21205, USA

Calorie restriction (CR) extends lifespan in a wide spectrum of organisms and is the only regimen known to lengthen the lifespan of mammals<sup>1–4</sup>. We established a model of CR in budding yeast *Saccharomyces cerevisiae*. In this system, lifespan can be extended by limiting glucose or by reducing the activity of the glucose-sensing cyclic-AMP-dependent kinase (PKA)<sup>5</sup>. Lifespan extension in a mutant with reduced PKA activity requires Sir2 and NAD (nicotinamide adenine dinucleotide)<sup>5</sup>. In this study we explore how CR activates Sir2 to extend lifespan. Here we show

that the shunting of carbon metabolism toward the mitochondrial tricarboxylic acid cycle and the concomitant increase in respiration play a central part in this process. We discuss how this metabolic strategy may apply to CR in animals.

Ageing in yeast is regulated by *SIR2*. Deletion of *SIR2* shortens lifespan and overexpression of *SIR2* extends lifespan<sup>6</sup>. Sir2 exhibits an NAD-dependent histone deacetylase activity that is conserved among Sir2-family members and is required for chromatin silencing and lifespan extension<sup>7–9</sup>. Recent studies show that *Caenorhabditis elegans* carrying extra copies of the *SIR2* orthologue, *sir-2.1*, also exhibit a longer lifespan<sup>10</sup>. The unusual NAD-requirement for the Sir2 deacetylase may link metabolic rate to silencing and lifespan<sup>11</sup>.

Calorie restriction can be modelled in yeast by reducing the glucose content of the media from 2% to 0.5% (ref. 5). We first extended our earlier findings by testing whether Sir2 is required for the extension of replicative lifespan by 0.5% glucose. As shown in Fig. 1a, growth in 0.5% glucose extended lifespan (~25% increase) relative to the normal 2% glucose, and deletion of *SIR2* prevented this extension. We also examined whether Sir2-dependent ribosomal DNA silencing is increased. As shown in Fig. 1d, cells grown on 0.5% glucose medium exhibited enhanced silencing (using a *MET15* marker integrated at the ribosomal DNA<sup>12</sup> as an indicator). This enhanced silencing, like the extension of lifespan on 0.5% glucose, required Sir2 function.

How does CR increase Sir2 activity and extend lifespan? As shown in Fig. 2a, glucose is metabolized to pyruvate, at which point the pathway bifurcates into respiration and fermentation<sup>13</sup>. Respiration oxidizes the glucose to CO<sub>2</sub> generating 28 ATP molecules per molecule of glucose, whereas fermentation to ethanol generates only two ATP molecules per molecule of glucose<sup>14</sup>. When glucose levels are high, energy is in excess and fermentation is preferred. When glucose is limiting, respiration is preferred and carbon is shunted to the mitochondrial tricarboxylic acid (TCA) cycle, thereby increasing electron transport and respiration<sup>13</sup>.

To investigate whether this metabolic shift toward respiration occurs under our conditions of CR, we measured oxygen consumption rates of cells in 0.5% glucose. Figure 2b shows that respiration of cells grown in 0.5% glucose was significantly increased (~2-fold) compared to that of cells grown in 2% glucose. As a further test for this metabolic shift, we used a strain lacking *HXX2*, which encodes one of three hexokinases that introduce glucose into glycolysis. Deletion of *HXX2* is expected to mimic the effect of growth in low glucose and has been shown to extend lifespan<sup>5</sup>. Transcriptional profiling of the yeast genome indicates a highly significant overlap ( $P = 3 \times 10^{-118}$ ) in the transcriptional changes caused by growth in 0.5% glucose and by deletion of *HXX2* (Fig. 3a). Similar to growth in 0.5% glucose, deletion of *HXX2* also increased the respiration rate significantly (~3-fold) (Fig. 2b).

Is the metabolic shift toward respiration required for CR-mediated lifespan extension? If so, elimination of electron transport ought to prevent the extension in lifespan. Thus, the gene encoding cytochrome c1, *CYT1*, was deleted, and lifespan analysis was performed (Fig. 2c). Calorie restriction failed to extend lifespan in the *cyt1Δ* mutant, suggesting that the metabolic shift toward respiration is necessary for lifespan extension mediated by CR.

We then investigated whether the metabolic shift toward respiration is sufficient for increased lifespan. Overexpression of the transcription factor Hap4 has been shown to cause a switch of metabolism from fermentation toward respiration<sup>15</sup>. Hap4 is expected to activate many genes involved in mitochondrial respiration<sup>16,17</sup>. Transcription profiling indeed showed that many of the genes that were upregulated more than 2-fold by Hap4 overexpression fell into this category (Fig. 3c; Supplementary Information Table 2). Overexpression of Hap4 significantly extended the lifespan (~35% increase) of cells grown in 2% glucose (Fig. 1b). Similar to CR, this extension required Sir2 (Fig. 1b). Hap4 overexpression also

† Present addresses: Longevity Inc., Medford, Massachusetts 02155, USA (M.K.); and CNRS UMR 5665, Ecole Normale Supérieure de Lyon, France (P.-A.D.).